

Landslides

DOI 10.1007/s10346-021-01817-z

Received: 20 May 2021

Accepted: 1 December 2021

© The Author(s) 2022

Hang Wu^{ID} · Mark A. Trigg^{ID} · William Murphy · Raul Fuentes^{ID}

A new global landslide dam database (RAGLAD) and analysis utilizing auxiliary global fluvial datasets

Abstract To address the current data and understanding knowledge gap in landslide dam inventories related to geomorphological parameters, a new global-scale landslide dam dataset named River Augmented Global Landslide Dams (RAGLAD) was created. RAGLAD is a collection of landslide dam records from multiple data sources published in various languages and many of these records we have been able to precisely geolocate. In total, 779 landslide dam records were compiled from 34 countries/regions. The spatial distribution, time trend, triggers, and geomorphological characteristic of the landslides and catchments where landslide dams formed are summarized. The relationships between geomorphological characteristics for landslides that form river dams are discussed and compared with those of landslides more generally. Additionally, a potential threshold for landslide dam formation is proposed, based on the relationship of landslide volume to river width. Our findings from our analysis of the value of the use of additional fluvial datasets to augment the database parameters indicate that they can be applied as a reliable supplemental data source, when the landslide dam records were accurately and precisely geolocated, although location precision in smaller river catchment areas can result in some uncertainty at this scale. This newly collected and supplemented dataset will allow the analysis and development of new relationships between landslides located near rivers and their actual propensity to block those particular rivers based on their geomorphology.

Keywords Landslide dam · Global fluvial data · Global-scale · Database

Introduction

The damming of rivers due to landslides and the following consequences pose great threats to people and facilities locally as well as in downstream areas. These landslide dams, which are effectively a subset of landslides that happen to block rivers, are reported in many areas around the world, almost exclusively in mountainous areas (e.g., Costa and Schuster 1988; Fan et al. 2020). The landslide dam (LDam) is an event that forms when the mass of a landslide or multiple landslides from the adjacent hillslopes, partially, or completely blocks the normal fluvial channels (e.g., Costa and Schuster 1988; George et al. 2019). Hundreds of LDams have occurred among the thousands of landslides generated in each triggering event, such as from earthquake or intense rainfall (e.g., Fan et al. 2012). Additionally, the economic and life loss of global LDam can accumulate into a considerable amount, as each event can cause the loss of millions of US dollars and many casualties (Dai et al. 2005; Tacconi Stefanelli et al. 2016; Fan et al. 2017). Moreover, LDams play an important role

as an interface connecting hillslope and fluvial channel systems in geomorphology (e.g., Korup 2002).

The primary consequence of LDams is the subsequent flood hazard resulting from the formation of a LDam. The potential impacts of LDams on ongoing floods can be divided into two parts: (1) upstream consequences, backwater floods, induced by rise of water level in the upstream area at the point of the LDam; (2) downstream consequences, downstream floods, mostly caused by the LDam failure, either by overtopping or breaching within short timescales (hours to days) (Zhang et al. 2016), depending on their dam material components (volume, texture, angle of repose, sorting), rates of seepage through the dam, and rates of LDam lake input and outflow (Costa and Schuster 1988; Korup 2004; Tacconi Stefanelli et al. 2018). In contrast to river flooding, which normally occurs after intense or prolonged precipitation or increasing snow-melt, the floods caused by LDam failures are more complicated to predict due to the rapid water release from the impounded lake when the dam fails, and the complexity of the LDam stability. The flowrate of dam-breach floods can increase river flows to many times typical flood flows experienced in a river system and can even reach a rate much larger than the flowrates of recorded flash floods (Perucca and Angillieri 2009). The impacts of dam-breach flooding can extend to broad areas since the distances of dam-breach floods can vary from 1 to more than 1000 km (Geertsema 2008; Evans et al. 2011; Macias et al. 2004). The flood wave generated when the landslide debris enters the fluvial channel can have a significant impact, such as a water level tens of meters above the mean water level (Wang et al. 2004), or a large peak discharge flood wave (e.g., 5900 m³/s reported by Dunning et al. 2006). These can have the potential to kill thousands of people in the downstream areas (Barla and Paronuzzi 2013).

The typical approach to study LDams currently is to establish a dataset of case studies and undertake analyses of the hazard-prone conditions of LDam formation from the empirical relationships using geomorphological parameters from the LDam and geomorphological records (e.g., Fan et al. 2012; Tacconi Stefanelli et al. 2016, 2018). The physical processes are very hard to capture accurately due to the lack of observational data. The formation of LDams is difficult to forecast, which makes systematic monitoring difficult. Even though LDam events are not uncommon, the records and datasets for this specific hazard are relatively sparse compared with its frequency of occurrence, especially on a global scale. The establishment of local, regional, or global LDam datasets has begun in earnest in the last few decades by collecting records from literature, field investigations, or remote sensing data (e.g., Costa and Schuster 1991; Fan et al. 2012, 2020; Tacconi Stefanelli

et al. 2016, 2018; Zhang et al. 2016). These previous studies have explored and proposed frameworks for data fields to be recorded in the LDam datasets, which are easy to use and update, even for non-experts, and have discussed LDam classifications, processes, origins, distributions, and stability on both a regional and global scale. Most of the records collected in these datasets were triggered by single events, mainly earthquakes (e.g., the 2008 Sichuan earthquake). These events result in a more comprehensive area coverage and data accessibility than single a LDam that may occur due an isolated landslide. There are some studies on the formation, stability, and short-term impacts of LDam that use these datasets (Ermini and Casagli 2003; Korup 2002; Fan et al. 2014), and most of them focus on studying the geomorphologic features of hillslopes, landslides, and the LDams.

However, the systematic understanding of the quantitative relationships between LDam formation and related geomorphological parameters on the global scale are still unclear due to the limited accessibility of valid records and parameters and the large variety of the local conditions. Most global LDam formation studies rely on descriptive analysis of case studies or quantitative relationships based on regional LDam studies or global landslide studies (Larsen et al. 2010; Tacconi Stefanelli et al. 2016, 2018). In previous LDam datasets, some of the geomorphological parameters of the landslides and blocked river valley came from empirical statistical relationships based on hydrological, geomorphological, or landslide studies (Evans et al. 2011), while others came from records or other accessible data sources (Tacconi Stefanelli et al. 2016, 2018; Fan et al. 2020).

To fill these gaps, in this paper, we develop a new global scale dataset of LDams, abbreviated as RAGLAD (River Augmented Global Landslide Dams), using a united spatial reference system and measurement units to allow a better understanding of the spatial distribution and characteristics of LDams and geomorphological conditions that might affect their formation on the global scale in relation to fluvial information. The records are collated from a wide range of data sources in multiple languages and geolocated with precise and accurate spatial information, where possible. The parameters of these records are then extended by linking the locations with recently available global fluvial datasets. This study is the first time that the combination of landslide databases with fluvial datasets has been presented. RAGLAD focusses on a global scale and allows us to explore and better understand the spatial distribution and geomorphological characteristics of LDams. For example, the relationships between geomorphological parameters, such as landslide volume and river width, are developed to explore the connection between geomorphological parameters and further reveal potential parameter thresholds for LDam formation from a global perspective.

Methods

Global landslide dam record collection

For a more comprehensive coverage in this dataset, the records in RAGLAD were collected from a wide range of sources: academic journal articles, government and institution reports, social media, and other available datasets in multiple languages (for more details, please see the supplementary materials in Appendix A).

The languages that were used most systematically for searching for relevant records were English, Chinese, and Japanese, although other languages related to the location of collected LDam records were also used, where available. A particularly careful focus of our data collection was in developing countries, where there was a distinct lack of records in previous studies. The measurement of geomorphological data is obtained directly from publications or extracted from published figures. An added difficulty is that current LDam records may include several events in one record. In order to create a unique LDam record for a particular location, where a LDam reference consists of multiple separate events and contain information that comes from different data sources, we need to precisely geolocate each LDam when its approximate location is available. During data entry, when conflicting data from various sources is presented for one record, data from field investigations and those records reported most recently to the LDam formation time are prioritized. We focused on more recent LDam events (in the last 1000 years) due to the sparsity of records and data from times before this, and because the reliability of the data is much less clear.

Previous LDam databases consist of similar geomorphologic parameters to landslides records, as well as parameters related to the LDam body, river valley and fluvial channel, impounded lakes, and the general information of LDam events which were helpful in building our database and locating original sources of information (Costa and Schuster 1991; Fan et al. 2012, 2020; Tacconi Stefanelli et al. 2016, 2018; Zhang et al. 2016; Zheng et al. 2021). The records in RAGLAD dataset contain information on the spatial and temporal information from dam formation to dam breach, dam materials, geomorphological characteristics, and dimension data of upstream catchments at the point of blockage, landslides and impounded lakes, and hydrographic characteristics of subsequent flood events and their consequences, including casualties and economic losses, as shown in Table 1. For a better understanding of the relationships between landslide types and the geomorphological characteristics of LDam formation, we applied the landslide definitions established by Hungr et al. (2014), including fall, topple, slide, spread, and flow, to recategorize the original landslide types from LDam record. Some descriptive and supplement information of the LDam events is also included to allow easier updating of the spatial location and geomorphological parameters in the future, if necessary.

On the global scale, 84% of valley blockage resulting from LDams were reported as being caused by rainfall and earthquakes (Schuster and Costa 1986). Similar result can be also found in the study by Zheng et al. (2021) with 50.4% cases induced by earthquakes and 39.3% by rainfall. Considering the triggering mechanism of landslides with large volume, the result is slightly different as 44.4% landslide were caused by rainfall, and 20.5% caused by earthquakes (Fan et al. 2020), so a smaller percentage. At that scale, localized effects that are also important cannot be considered. However, on a local scale, the fluvial erosion of channel beds/banks and erosion processes that change the condition of hillslopes are known to influence the hillslope stability (Golly et al. 2017). Based on RAGLAD, triggering processes of landslides that have formed dams can be summarized into three major categories: (1) meteorological triggering processes, including meteorological events, such as storm, snowmelt, and

Table 1 The information field of LDam records (for more details, check with [Supplemental Materials](#))

Criteria	Information/parameters	Format	Unit/category	Description
Basic information and location	ID	Number	-	The unique recording index of events in this dataset
	Name	Text	-	The local name of LDam in English
	Name in the original language	Text	-	The local name of LDam in their original language
	y	Number	-	Location—Latitude (WGS1984)
	x	Number	-	Location—Longitude (WGS1984)
	Location	Text	-	Location description of where the LDam event occurred
	Country/region	Text	-	Country or region of origin
Time	Formed time	Time/Text	yyyy/mm/dd	Time of formation
	Dam failure time	Text	-	Time of dam collapse
	LDam status	Text	Failed/existing/unknown	Status of LDam
	Failure mechanism	Text	-	Mechanism of dam collapse if known
	Overflow/flood Time	Time	-	Time of collapse or overtopping of an existing dam which causes subsequent flood
	Duration from formation to flood (lake life)	Text	-	The time from dam formation to failure or time when the impounded lake disappeared
Catchment	Drainage area	Number	km ²	The upstream drainage area of the river channel at point of the LDam
	River width	Number	m	The width of the river channel where the LDam occurred
Landslide	Landslide Subcategories	Text	-	Landslide classification in original pieces of literature
	Type of movement	Text	Uncategorized/ slide/fall/flow/topple/complex	Landslide movement categories (Hungre et al. 2014)
	Landslide area	Number	m ²	The surface area of the landslide
	Landslide-elevation difference	Number	m	The elevation difference between the crown and toe of the landslide
	Landslide length	Number	m	The main body length of the landslide that formed the dam
	H/L ratio	Number	-	The ratio of landslide height divided by length for measuring the mobility of landslides debris (Iverson 1997)
	Landslide volume	Number	10 ⁶ m ³	The volume of landslide that forms the LDam

Table 1 (continued)

Criteria	Information/parameters	Format	Unit/category	Description
LDam	LDam-type	Text	-	Classification of LDam (Costa and Schuster 1988)
	Dam materials	Text	-	Grain size and lithology of LDam materials
	Reported cause	Text	-	Landslide triggering processes described in original works of literature
	Interpreted cause	Text	Meteorological/geological/hydrographical triggering processes (with detailed categories)	Categories of landslide triggering processes summarized in this study
	Dam height	Number	m	Height of landslide deposit forming the dam
	Dam length	Number	m	Length of LDam (across the valley)
	Dam width	Number	m	Width of LDam (along the valley)
Impounded lake	Impounded lake length	Number	km	Length of an impounded lake dammed by a landslide
	Impounded lake volume	Number	10 ⁶ m ³	The volume of an impounded lake dammed by a landslide
Subsequent flood	Mean flow velocity	Number	m ³ /s	Mean flow velocity of river under normal flow conditions
	Peak flow velocity	Number	m ³ /s	The peak flow velocity of flood related to LDam formation and failure processes
Consequence	Casualties	Text	-	Number of deaths/injuries
	Economic loss	Text	-	Economic losses including properties and infrastructure
References	-	Text	-	References used for recording LDam events (Sources of information)
More details	-	Text	-	Related details that were not mentioned above

intense precipitation, and the alternation of the seasons, when the temperature and humidity change sufficiently; (2) geological precondition and triggering processes, including the geological background that is prone to LDam occurrences, such as layers and lithological characteristic of the bedrocks on the hillslopes and long-term tectonic movement, infiltration towards potential or current landslide bodies that could alter the shear strengths of surface materials and induce potential landslides, and geological hazards such as earthquake, volcano eruption, and landslide reactivation; and (3) geomorphological triggering processes, such as the fluvial geomorphology changes caused by fluvial erosion processes at the base of a hillslope, alluviation, or flood hazards.

Geolocating LDam records

The precise and accurate spatial location of LDam records is crucial for further geospatial or geomorphological analysis and to allow linking of parameters from other data sources (Fan et al. 2020). However, most of the spatial information in the records in current global datasets was recorded as approximate location descriptions, without precise spatial coordinates. Hence, these datasets cannot be used to link records with other geolocated data. There are three key challenges in recording the precise spatial coordinates of records: (1) LDam can form and fail in a very short time and thus its precise location can escape being recorded; (2) older LDam events were not

recorded with very precise locations because the locations were derived from the geomorphological or sedimentary relics, which may not be clearly presented in modern terrain (Tacconi Stefanelli et al. 2016); and (3) collating data recorded in different data formats, inconsistent units with vague and patchy spatial information impedes the process of assigning precise coordinates and can result in the imprecision of spatial information.

In this study, the records were geolocated individually by georeferencing, projection transformation, or based on the geomorphological information and location description provided in the original data sources. To improve the spatial precision of the records, we visually scanned the target area using Google Earth to find the geomorphological signature of the landslides that had created the dams. These signatures include landslide scarps, the extreme color differences on the ground caused by surface vegetation changes or the loss of soil cover, hazard mitigation infrastructures, and existing LDam bodies and impounded lakes, and then matched the approximate location with the description and images reported on social media or local reports to pin down the precise spatial location of LDam records (for more details, check with [Supplementary Materials Appendix B](#)).

Appending the data from the global fluvial dataset to landslide dam records

Even though the number of LDam records increased during the past decades, some of the data, especially the geomorphological data, such as river width and drainage area at the point of the LDam, is not valid in every information field for each record. The LDam body and its deposits may be removed by erosion, in some cases even within a few hours after its formation and thus sometimes

Table 2 Data entry completeness of specific critical parameters. Bold values are improvements after geolocating and adding Global Fluvial Datasets

Parameters	Completeness	Completeness after geolocating and adding GFD
Name	47.1%	47.1%
y (latitude)	68.1%	85.5%
x (longitude)	68.1%	85.5%
Country/region	100%	100%
Location (text)	89.6%	89.6%
Formation time	90.2%	90.2%
Type of landslide movement	76.7%	76.7%
Drainage area	71.7%	85.5%
River width	38.3%	85.5%
Landslide area	39.0%	39.0%
H/L Ratio	51.0%	51.0%
Landslide volume	70.3%	70.3%

it is impossible to record their dimension by field investigations. When most records are geolocated, linking accessible parameters from other data sources by spatial proximity becomes possible. This allows us to complete some records that lack valid data on the

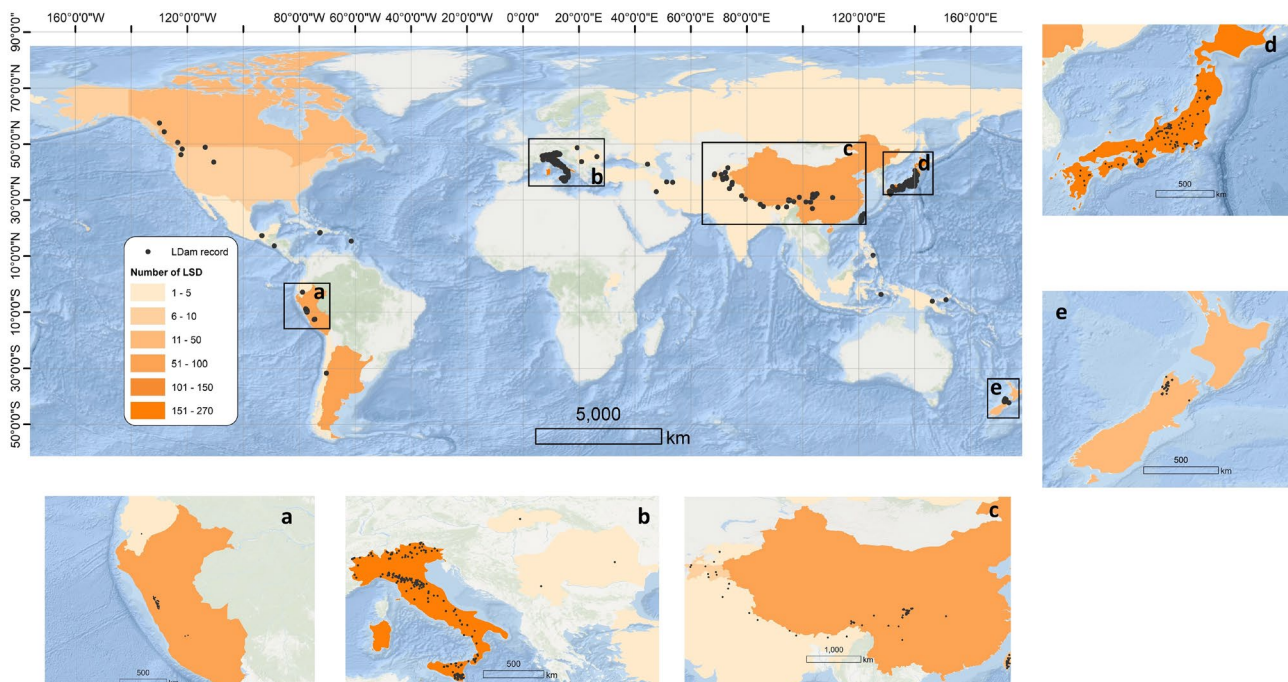


Fig. 1 Spatial distribution of LDam records with precise geospatial locations in RAGLAD (a. Peru; b. Italy and southern Europe; c. Himalaya areas; d. Japan; e. New Zealand)

fluvial system parameters, such as upstream drainage area and river width. In parallel, with the development of digital elevation models (DEM) in recent decades, the geomorphological parameters can be easily obtained. Therefore, linking the geomorphological data from the validated global fluvial dataset can be a valuable approach.

Global fluvial datasets (GFDs) have made significant progress in recent decades. Lehner et al. (2006) released HydroSHEDS (Hydrological data and maps based on Shuttle Elevation Derivatives at multiple Scales) derived primarily from elevation data from the Shuttle Radar Topography Mission (SRTM) at the spatial resolution ranging from 3 arc-second (~90 m) to 5 min (~10 km). Yamazaki et al. (2014) developed a new global river width database to provide fluvial data sources with global coverage for data supplemented with river widths. Allen and Pavelsky (2018) completed the first global compilation of river planform geometry based on the Landsat images. Linke et al. (2019) published the HydroATLAS database providing the descriptive hydro-environmental information for worldwide watersheds and rivers at 15 arc-second (~500 m) resolution. In the same year, the first global dataset including mean annual flow, river width, slope, meander wavelength, sinuosity, and catchment area was created from river centrelines derived from Landsat images and Shuttle Radar Topography Mission DEM (Frasson et al. 2019). Yamazaki et al. (2019) published MERIT Hydro, a new global flow direction map at the resolution of 3 arc-second (30 m) derived from the latest elevation and waterbody data. Among all these GFDs, we selected the raster-based MERIT Hydro dataset for data assembling

of drainage area and river width data because it reduced the vegetation biases from the elevations of satellite-derived DEMs, which can lead to an imprecise water body representation in forest areas, and includes the correction of many other DEM errors (Yamazaki et al. 2019). The global empirical relationship between river width (W) and drainage area (A) achieved from the study of Frasson et al. (2019) was also selected for calculating the river width for further comparison (Eq. 1), because the MERIT Hydro does not cover all the smaller catchments. We compare the fluvial data from original records with that derived from GFDs by retaining the data from original records and appending all the valid data from the GFDs to evaluate the assembled performance of these different sources.

$$W = 9.68A^{0.32} \quad (1)$$

Results

Observed trends in the landslide dam database

In total, 779 LDam records were compiled from 34 countries/regions. The locations of the records are clustered in the mountainous areas around the world, especially in the areas including European Alps (Tacconi Stefanelli et al. 2016), Rocky Mountains (Costa and Schuster 1988; Clague and Evans 1994), Andes Mountains (Hermanns et al. 2011; Tacconi Stefanelli et al. 2018), Pamir Mountains (Storm 2010), Himalayas (Evans et al. 2011), the eastern edge of Tibet Plateau (Yin et al. 2009; Xu et al. 2009;

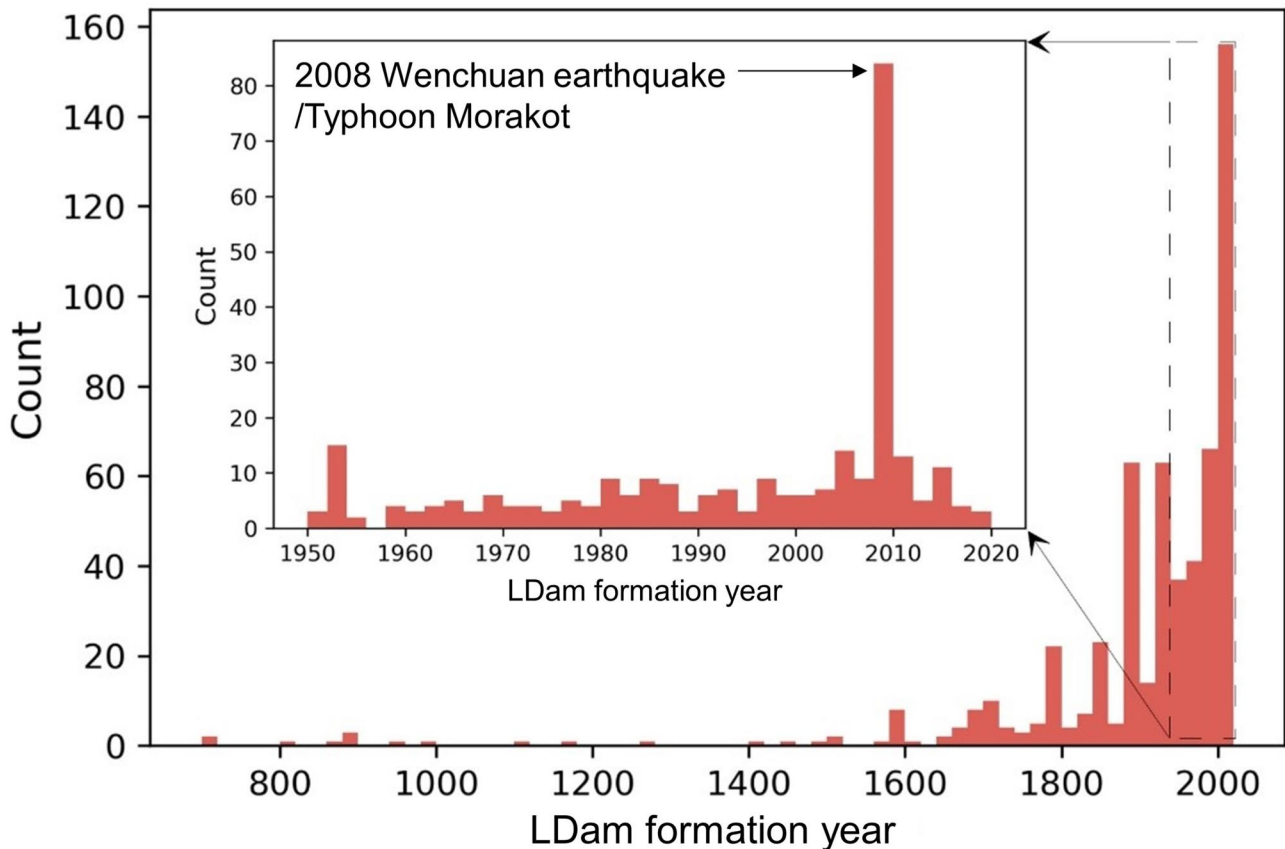


Fig. 2 Formation time trend of LDam event, inset shows the last 70 years in more detail

Fan et al. 2012), and some mountainous areas on islands (Nash et al. 2008) (Fig. 1). In terms of spatial information of the new database, 85% of the records (666 out of 779 records) contain location information with a precision of approximately 0.01 degree (~1 km) and 583 records (~75%) have a precision better than or equal to 0.001 degree (~100 m) after geolocating processes. The influence of geolocating in the data completeness is shown in Table 2 (for all parameters, see the supplementary materials in Appendix D). The diversity of data availability in different countries due to funding, expertise availability, and disaster management policies strongly affects the spatial data distribution. For instance, most of the current LDams are recorded in developed countries, such as the USA, Canada, Italy, and Japan, and some developing countries with plenty of researchers in this study topic (e.g., China, and Argentina).

The recorded date of LDam formation shows a clear increasing trend in the number of records during the past 1000 years, with the highest number in the last 20 years (Fig. 2). This increase is probably due to the greater amount of landslide research and the growing interdisciplinary interest in multi-hazard research, particularly in mountainous areas, rather than an actual increase in events. LDams that occurred in the past may have only been recorded occasionally, and this leads to the under-representation of LDam numbers in the

past (Tacconi Stefanelli et al. 2016). Extreme hazard events such as the 1783 Calabria earthquake in Italy, the 1889 Totsugawa Flood in Japan, the 2008 Sichuan earthquake in China, and Typhoon Morakot in 2008 have contributed to the notable peaks in the LDam formation time trends.

Landslide dam triggering processes

The database records show that the LDams were triggered by multiple factors. Among the 506 LDams with the recorded categories of landslide triggering processes (Fig. 3), 314 were induced by extreme geological events, 151 were triggered by weather events, and 65 were directly caused by fluvial landform system changes. It must be noted that a single LDam record may have more than one triggering factor. The results indicate that the triggering processes of geology and meteorology dominantly control the formation of LDam around the world as 62% of LDams are induced by geological triggers, 30% of LDam records caused by meteorological triggers, and 13% LDams are caused by geomorphological triggers. This finding is similar to that by Schuster and Costa (1986), who that found more than 84% of global natural dams were triggered by factors related to earthquakes and precipitation and Zheng et al. (2021) with 50.4% of

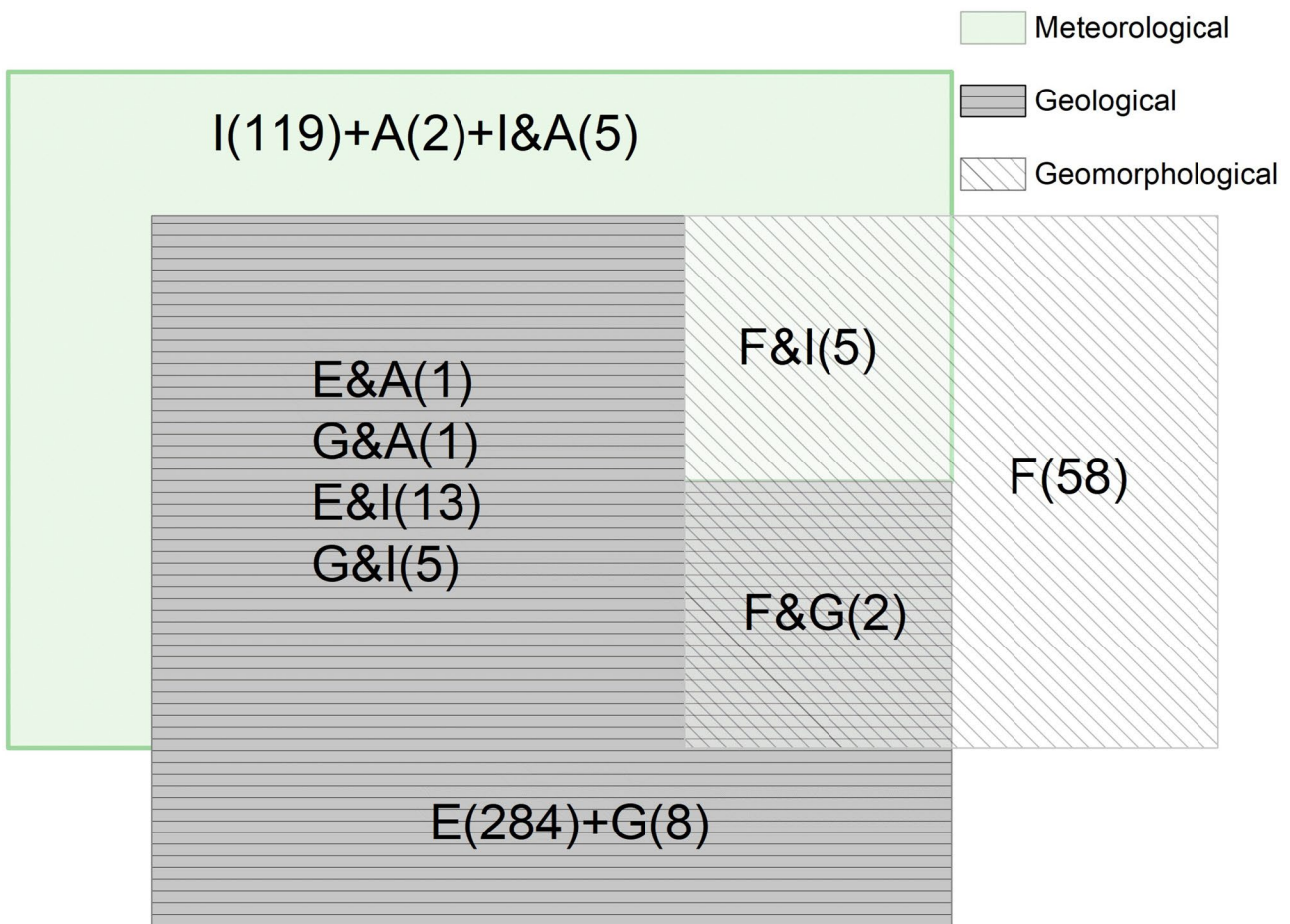


Fig. 3 Venn diagram of landslide triggering processes categories (A, alternation of season; I, instant weather event; E, extreme geological hazard; G, geological background; number followed the categories is

the number of records with specified landslide triggering processes categories)

landslide triggered by earthquakes and 39.3% induced by rainfall. A slight difference can be found for long run-out distance landslides according to Fan et al. (2020), who found that 20.5% of landslides were triggered by earthquakes and 44.4% were induced by rainfall. However, it is not clear that the LDam triggering processes result is due to the actual hazard occurrence or some of these triggers happen to attract more research attention. Additionally, these triggering processes can place a strong bias on the dataset by producing a lot of landslides and landslide dams at once.

Geomorphological characteristics of landslide dam records

As observational data of the LDam formation processes in action are rarely available, summarizing the geomorphological characteristics of upstream catchments, and the landslides from records can be helpful when considering the geomorphological conditions prone to LDam formation. We consider here the 4 geomorphological characteristics of LDams in the RAGLAD database, including drainage area (at the point of LDam), river width (at the point of LDam), the ratio of the landslide drop height to landslide runout distance (H/L ratio), and landslide volume (Fig. 4), which can

include the geomorphological conditions from the blocked river channel and its triggered landslide from the adjacent hillslopes. This allows us to study two specific factors: (1) where LDams occur along the course of a river, and (2) what kind of landslides are likely to dam a river.

Based on the geomorphological data of the blocked river channel, the LDam records occurred more frequently in the upstream areas of river systems where the slopes tend to be steeper and therefore, more likely to fail. The geomorphological characteristics of the drainage area at the point of valley blockage shows an exponential distribution, with most records having a drainage area less than 500 km² (Fig. 4-a). Strahler stream order is used in river morphology as a measure of the stream network connectivity. The most upstream reaches of a river are classed as order 1 and when these join another stream of order 1, then the reach becomes an order of 2, and this continues downstream with ever increasing stream orders (Geological Survey 1965). The range of stream orders for the records vary from 1st to 5th order. This large number of low stream orders, as well as the smaller catchment areas, confirms that LDams usually occur in upper river catchment areas. The data distribution of river width suggests that the LDam is more likely to occur

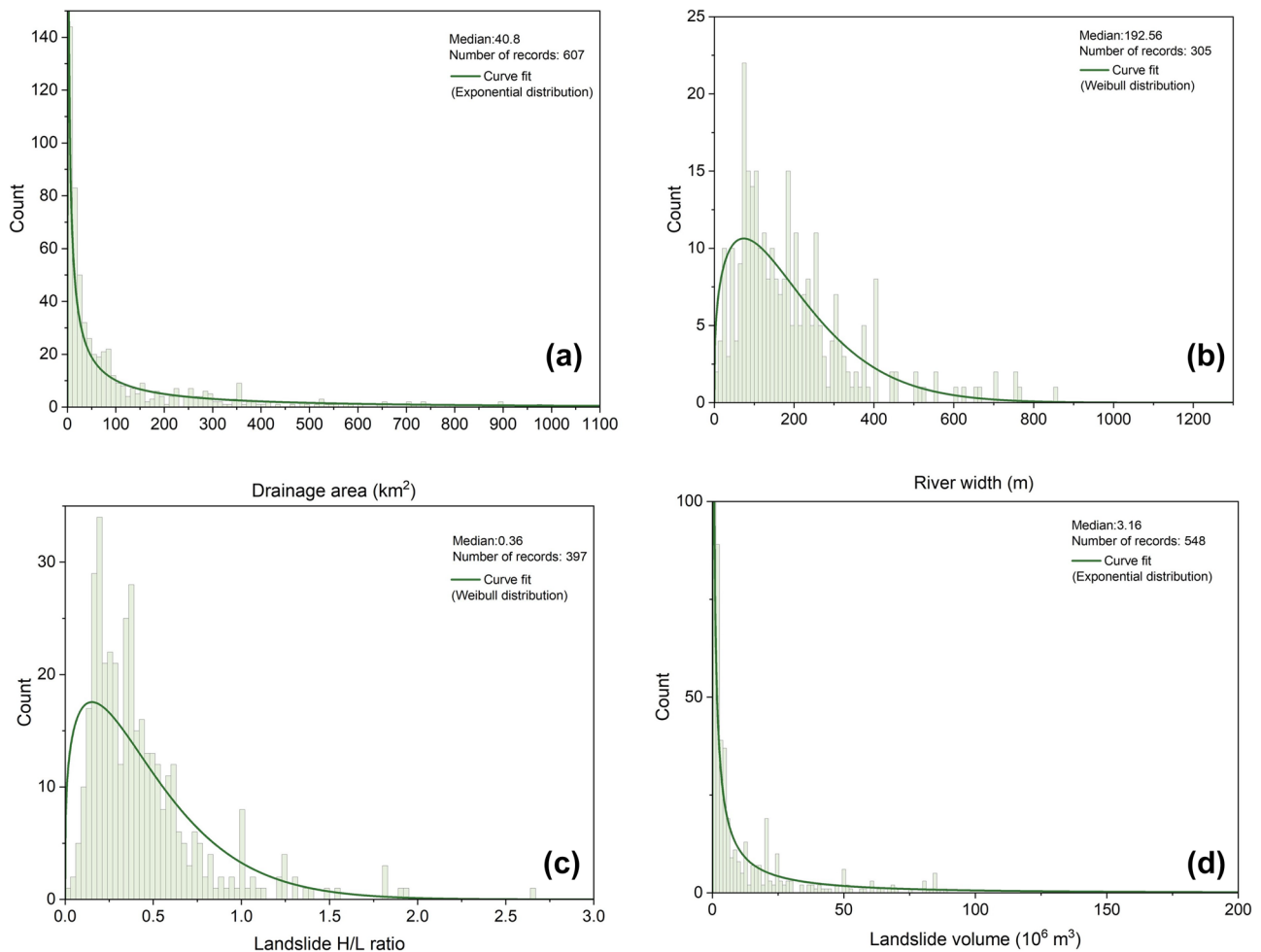


Fig. 4 Data distribution of geomorphological parameters of LDam records: (a) drainage area; (b) river width; (c) landslide H/L ratio; (d) landslide volume

in smaller rivers from the range of 0 to 300 m width, as expected, which is similar to the result shown for the drainage area distribution (Fig. 4-b).

The geomorphological data distributions of landslide dimension parameters indicate that a larger volume and longer run-out distance of a landslide can contribute to the LDam formation prone conditions. However, the condition depends on specific landslide types and LDam locations. The H/L ratio is a popular parameter for measuring the mobility of a landslide, even though it is still under discussion within long-runout landslide literature (Iverson 1997; Legros 2002; Shanmugam and Wang 2015), and its mechanical meaningfulness as a description of friction has been refuted several times (Hsü 1975; Davies 1982; Dufresne and Geertsema 2020). The result of the landslide H/L ratio shows a Weibull distribution with most H/L ratios concentrated in the range from 0.12 to 0.6 and this indicates the contribution of relatively long run-out landslides to LDam formation. Typical landslides have a H/L ratio smaller than 0.5, with some well-studied examples reaching a value of 0.1 to 0.2 (Iverson 2015); this work on debris flows demonstrates that the run-out distance can be considerable. For example, the debris flows, debris avalanches, and rock slides in west central British Columbia have an H/L value between 0.1 and 0.5 (Geertsema et al. 2009). Scheidegger (1973) described a general trend of a reducing H/L ratio with an increase in volume and suggested that some obstructed mudslides and earth flows will have a lower H/L ratio than other landslides. The fact that the majority of landslide movement types that formed

LDams include slide (> 28%), complex (> 24%), and flow (19%) can affect this data distribution because the H/L ratio is highly influenced by the landslide type.

The data distribution of landslide volume from landslides that block the valley reveals an exponential distribution, with 68% data concentrated in a volume of less than 10 million cubic meters. Among all the data, it is interesting to note that for more than 17% of LDam records (132 out of 779 records), landslides with a small volume (< 1 million m³, as a volume threshold of long run-out rock avalanches/slides defined and applied by Glastonbury and Fell 2008; Evans et al. 2011; Davies and McSaveney 2012; Robinson et al. 2015; Chunyuk et al. 2020; Fan et al. 2020) also plays an important role in contributing to the total amount of records.

The data distribution of landslide geomorphological characteristics could be the result of various reasons:

- 1) the proportion of larger landslides is relatively small in LDam studies. However, compared with those in general landslides studies, the landslides causing LDams with a volume larger than 1 million cubic meters account for a larger proportion of the total (75%). In the study of Guzzetti et al. (2009), the landslides with a large volume took up approximately 29% of 667 landslides in Umbria, central Italy. In the national scale landslide dataset of Slovenia, the large volume landslides account for approximately 0.4% of the total (Komac and Hribernik 2015);

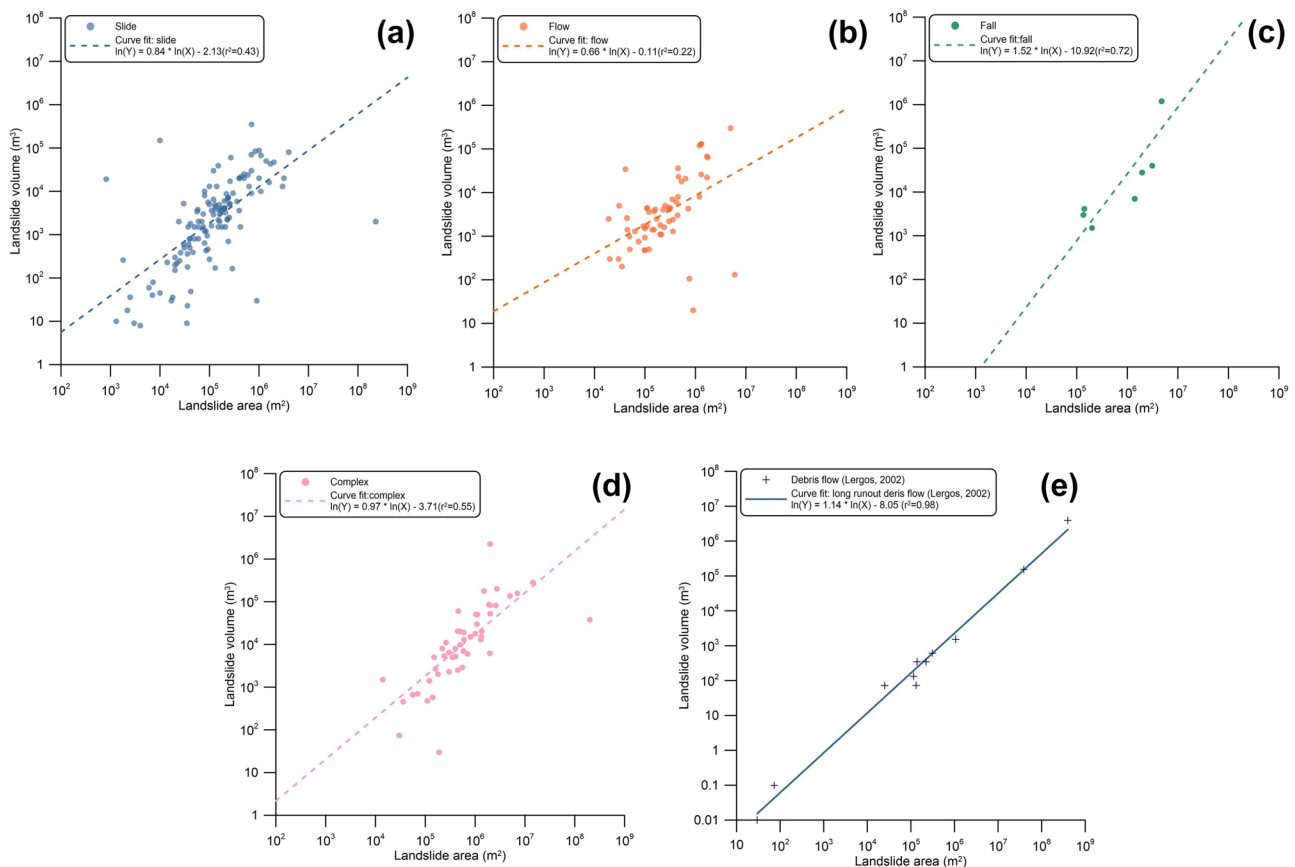


Fig. 5 Correlation between landslide volume and landslide area for 260 records with valid data, categorized by landslide types. **a** Slide. **b** Flow. **c** Fall. **d** Complex. **e** Long run-out debris flow (Legros 2002)

- 2) the result is affected by both the river width and H/L ratio distribution result, because to block a larger river width requires a larger volume of landslide material, which may require a longer landslide runout distance from a lower H/L ratio. However, from previous studies, the increase in L/H (opposite to H/L ratio) with increasing volume of landslides was not observed for both small and large landslides (Roback et al. et al. 2018) and Okura et al. (2003) reported that there is no correlation between the volume and H/L ratio for shallow landslides under the volume of 10^3 – 10^4 m³;
- 3) The result could be affected by landslide types and the actual volume of the LDam blocking the river. For some landslide types, the volume that actually blocks the river is much smaller than the total landslide volume ($\sim 10\%$ for the cases covered in Miller et al. 2018).

Empirical relationships between parameters

The relationship between landslide volume and landslide area, based on the LDam records collected in this research, is shown in Fig. 5. As landslide type is a principal factor for determining the relationships between landslide runout and volume (Legros 2002), we have measured the relationships grouped by different landslide movement types. As shown in Eq. 2, the relationship between landslide area and volume is presented as a scaling relationship. Previous studies (Guzzetti et al. 2009; Larsen et al. 2010; Fan et al. 2012, 2014) have shown its applicability to a broad range of landslide types.

$$V = \alpha A^{\gamma} \quad (2)$$

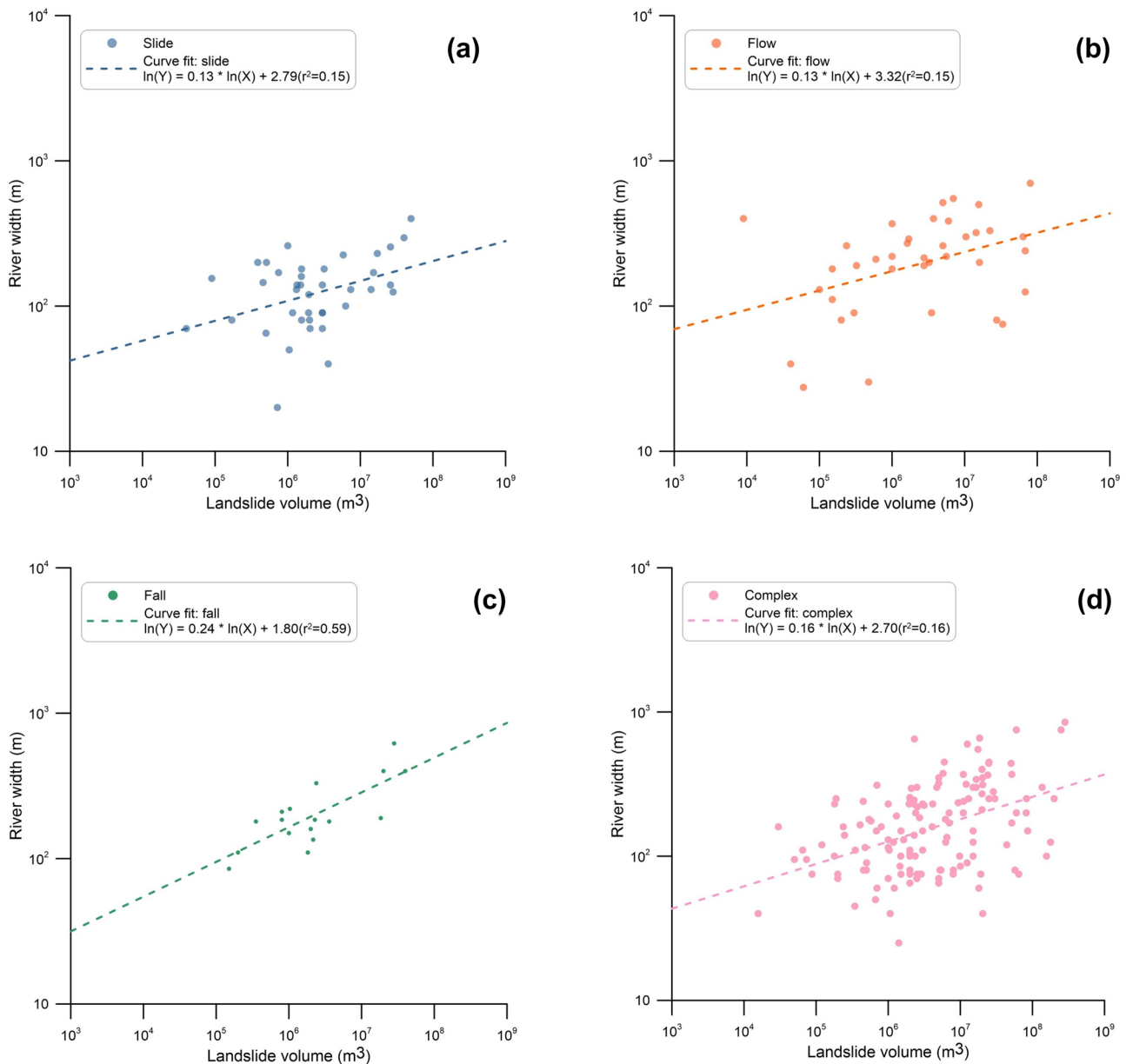


Fig. 6 Correlation between landslide volume and river width (as defined in Table 1) for 250 records with valid data, categorized by landslide types. **a** Slide. **b** Flow. **c** Fall. **d** Complex

where V is the landslide volume (m^3), α is the intercept, A is the landslide area (m^2), and Y is the scaling exponent. A previous study by Larsen et al. (2010) established a global prediction equation of the exponential relationship between landslide volume and landslide area that was based on more than 4000 landslides in both soil and rock types collected globally. The value of Y derived for landslides in soil is 1.1–1.3. For landslides which occurred in rock masses, the range of values is 1.3–1.6. This relationship has been directly applied to both landslide and LDam studies on the regional scale for calculating landslide volumes (Fan et al. 2014; Tacconi Stefanelli et al. 2018). The smaller scaling exponent of landslides that dam the river, with a range from 0.66 to 0.97, indicates that these landslides typically have smaller volumes compared to landslides more generally (i.e., including those that do not cause LDams). This situation could be due to the erosion depth of landslides that dam rivers being shallower or having steeper slopes comparing with the general landslides. However, as the scaling exponent varied with slope materials in the V-A scaling exponent study in global landslides (Larsen et al. 2010), it is common to expect that most of the coefficients of determination (r^2) in these relationships are relatively low (< 0.5) because of the vast combinations of landslide mass materials, patchy data sources, and different triggering mechanisms of landslides.

To determine whether a landslide can actually form a LDam, it is vital to know the empirical relationship between landslide volume and river width from current records. The empirical relationships

within the geomorphological parameters, especially the relationships between landslide volume and area, were applied in establishing geomorphology indexes for evaluating the LDam formation probability and stability (Tacconi Stefanelli et al. 2018). The correlation between landslide volume and river width revealed similar relationships within the categorized landslides that formed the LDam, but the relationships are not clear, with a lot of data noise (Fig. 6). LDam formation index from previous research, such as Morphological Obstruction Index (MOI), also applied the relationship between valley width and landslide volume (Tacconi Stefanelli et al. 2016). However, we have to point out that there is a difference between valley width and river width. River (channel) width is based on the mean annual flow (Frasson et al. 2019), while the valley width derived from the valley morphology system rather than just the river, so valley width is always wider than river channel width. One of the reasons for the data noise may come from the uncertainties resulting from the original records. Nonetheless, although a correlation between landslide volume and river width is not possible, it still reveals a potential threshold for LDam formation (Fig. 7). Only one outlier from the dataset in Italy (Tacconi Stefanelli et al. 2016) is above this threshold line, and it dammed a valley of 400 m width with 9000 m^3 debris. No further information was found regarding this outlier. The threshold can be applied to explore the LDam formation prone areas where landslides can generate sufficient volume of mass to block the river: i.e. the minimum landslide volume that forms a LDam can be calculated from a given river width.

Fig. 7 The potential threshold of LDam formation by the relationships of landslide volume and river width

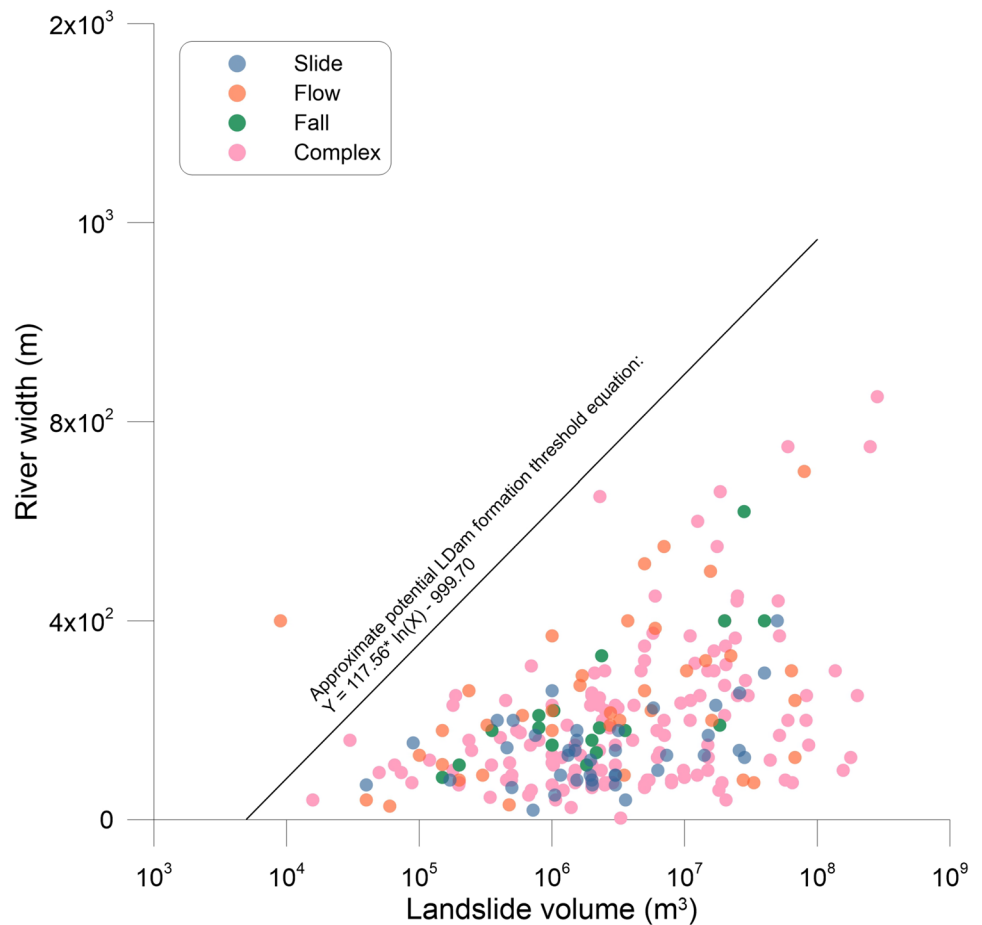
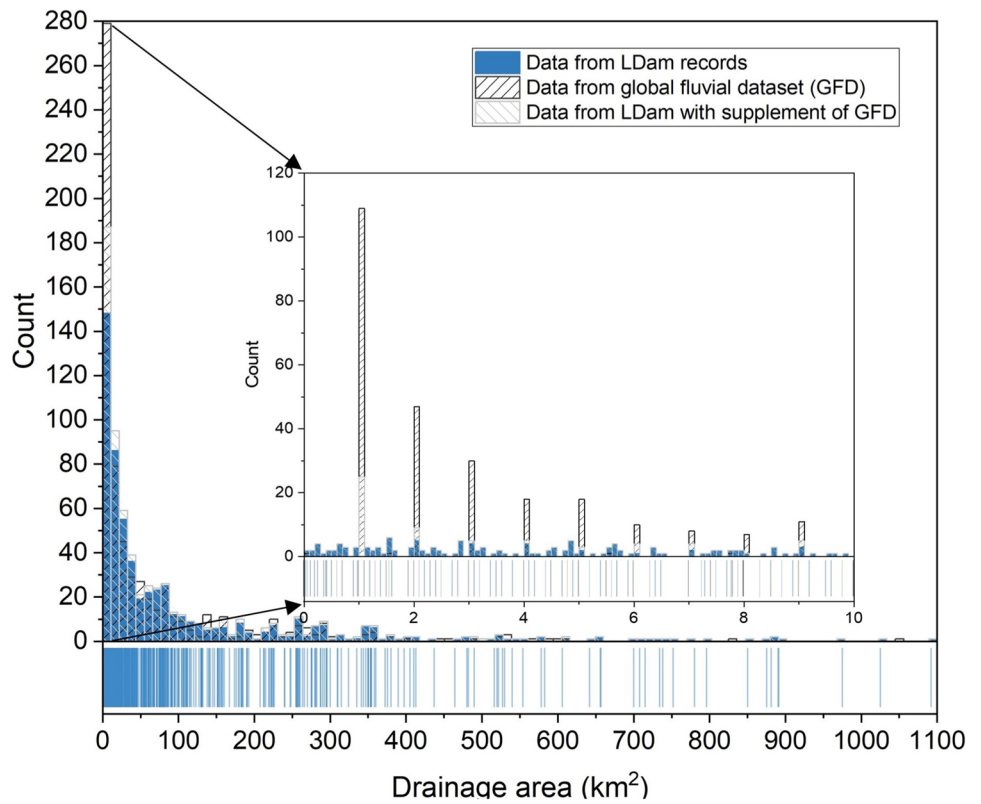


Fig. 8 Data distribution of drainage area from RAGLAD, GFD, and RAGLAD with the supplement of the GFD (bin interval of 10), inset shows the data distribution in the first bar in more detail (bin interval of 1)

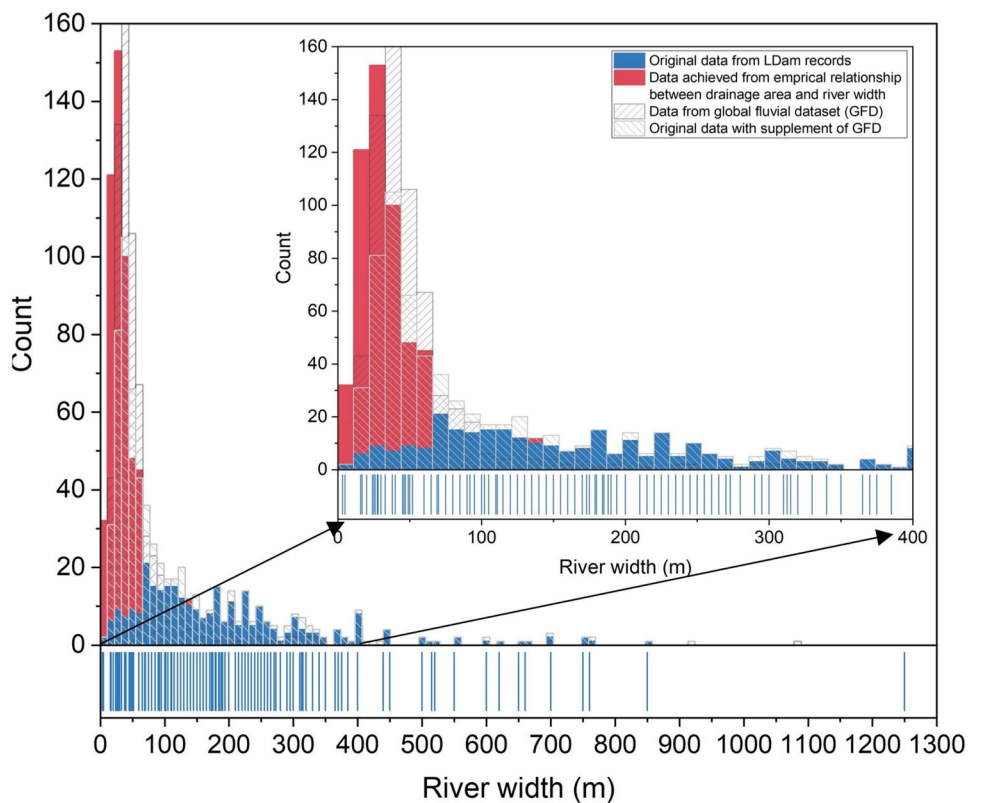


Global fluvial datasets parameter results

The data distribution results of the drainage area when combined with the global fluvial datasets (GFD) reveals three similar Weibull

data distributions of drainage area developed from the following: (1) the original LDam records only; (2) GFD data only; and (3) RAGLAD dataset combined with the GFD data (Fig. 8). The drainage area data collected from the GFDs contain more values for the areas less than

Fig. 9 Data distribution of river width from RAGLAD, GFD, and RAGLAD with the supplement of GFD and data derived from empirical relationship to drainage area; inset shows the data distribution of river width from 0 to 400 m



20 km², which are lacking in the original LDam records. When zooming into these upstream catchments with smaller areas, we can also see that the data gathered from GFD only shows as integer values (due to the GFD format) and this could lead to a larger data value difference and distribution in narrower rivers (drainage area < 20 km²). In contrast to the very similar distributions for the drainage area, the distributions of river width from various data sources are more diverse (Fig. 9). The data difference exists mainly in the rivers with a width less than 50 m, whose width data were mainly collected from the GFDs. Therefore, one of the most significant reasons for the difference between drainage area and river width is the amount of valid data between these 2 parameters; there are 627 records containing valid data on drainage area while there are only 303 records that have a valid river width values from the original records.

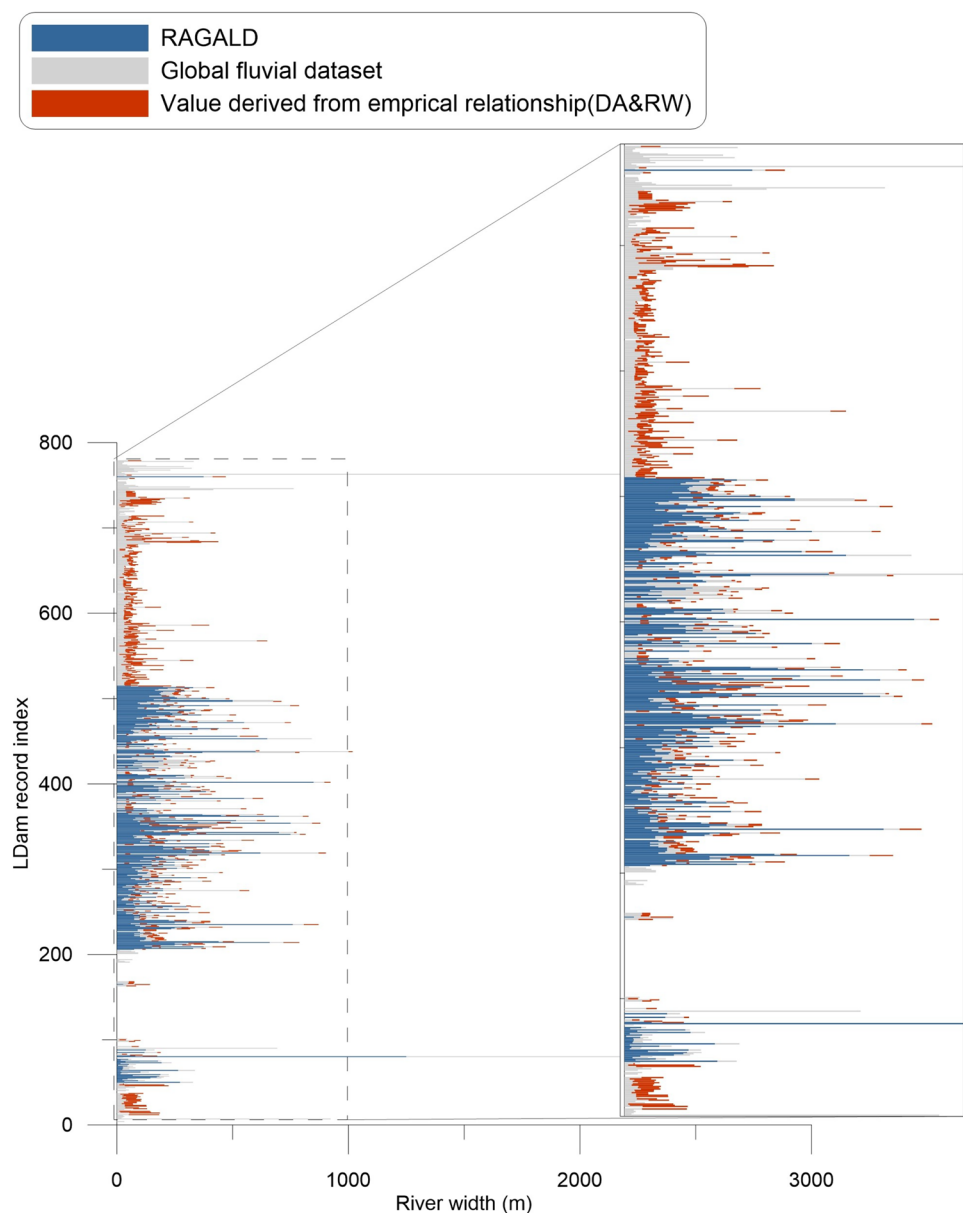
Both the data supplement of river width from the GFDs and the empirical relationship between river width and drainage area fill a significant data gap in the current LDam datasets, particularly

in the range of river widths less than 100 m (Fig. 9). The data distribution is slightly different after data combination, but is still very similar, but with differences concentrated at the smaller river scales where there is the most difference in the data. The data gap between LDam records and GFDs is concentrated in small rivers and catchments, which also raises the need to improve the GFD performance in smaller catchments. We also compared the data extracted from different data sources in each record (Fig. 10). For those LDam records with a valid river width value, the GFD data gathered from MERIT hydro performs better than river width data estimated by drainage area simply using the empirical relationship of drainage area and river width (Frasson et al. 2019).

Discussion

We have presented the data distribution and parameter correlation results achieved from our new-established RAGLAD dataset. Record gaps of river morphology parameters have been filled,

Fig. 10 River width data comparison among LDam records, GFD, and data achieved from the global W-A empirical relationship (Eq. 1 from Frasson et al. (2019))



where possible, with values derived from global fluvial datasets. There is some obvious data noise when correlating geomorphological parameters based on original LDam records. The results also showed that obtaining data based on data combination with GFD results in better performance, comparing with calculating a specific parameter value based on established generalized global empirical relationships. However, it is also notable that the data combination results can affect the data distribution when the valid data in original records are limited (less than 50% of records with valid data). Our result indicates that although the GFD can be a better supplement source for current records than supplying data based on empirical relationships from other geomorphological parameters, there are also some uncertainties that exist that affect the data combination result, and this can reduce the accuracy of resulting data.

A possible reason for inaccuracies could be the potential data recording bias and uncertainties caused by original LDam records, including the inaccuracy and imprecision of spatial information or geomorphological data occurring during the recording process. Depending on the quality of data sampling and age of the event, the spatial inaccuracy and imprecision of the records can become one of the most important sources of uncertainty in the data when recording dimension data from other data sources, because it can link inaccurate data to the record (Tacconi Stefanelli et al. 2016). Some of the geomorphological parameters from the records, such as landslide volume and landslide area, were estimated based on the empirical relationships or achieved from remote sensing data, because the data cannot be obtained before the LDam disappears (Costa and Schuster 1988; Fan et al. 2020). The records from RAGLAD came from various landslide types and sizes and this can also lead to uncertainty in the mechanism of LDam, if it is a result of more complex combined processes. Since a lot of records from the RAGLAD dataset are clustered in the smaller catchments and the fact that smaller catchments have less persistent river flow fluctuations (Hirpa et al. 2010), it is possible to speculate that there may be a larger data difference between obtained data from the literature

and actual event investigation data because of the temporal gap. Inconsistency in the terminology used during the data acquisition of LDams and landslides from different works of literature can lead to some confusion. For instance, the volume of the landslide may refer to either the volume of the landslide or the total landslide excluding the LDam body (Korup 2004), and the length and width of a LDam body from different studies could be used interchangeably (Costa and Schuster 1988). Additionally, the data collected from the various data sources or recorded in different data formats, inconsistent units, and spatial references can increase the uncertainties of data collation.

As the GFD datasets contain global-coverage hydro-morphological data, they can provide a reliable source for supplementing the original records. Therefore, another possible reason that can cause inaccuracy of data entries can also come from the GFD datasets themselves. Although GFDs have been developed over the past decade with a more precise representation of river networks, there remain some limitations within the current GFDs: (1) GFDs generally apply single flow direction methods, such as the D8 algorithm, for generating the flow direction map and thus they contain no channel bifurcations because the flows in the upstream areas tend to become concentrated to a distinct single flow direction (Tarboton 1997; Seibert et al. 2007); (2) most of the geomorphological characteristics or relationships between fluvial parameters from GFDs were recorded with mean annual values, and there may exist a temporal gap between the time of LDam formation and the time of data collection and thus result in the data difference between GFD and actual LDam events; (3) small rivers are still poorly represented due to the limitation of horizontal spatial resolution of the DEMs that these GFDs are derived from (pixel size of raster grids) (Yamazaki et al. 2014). These limitations of current GFDs can lead to the underestimation or overestimation of related fluvial parameters. For example, Fig. 11 (a) shows an example of the situation when the GFD data did not contain river channels where some records were located. Figure 11 (b) shows the landslides in Peilong valley that reoccurred in the same place several times in the 1980s (Li et al. 2020), which actually blocked a tributary nearby instead of the mainstream presented in the GFD data, so the data

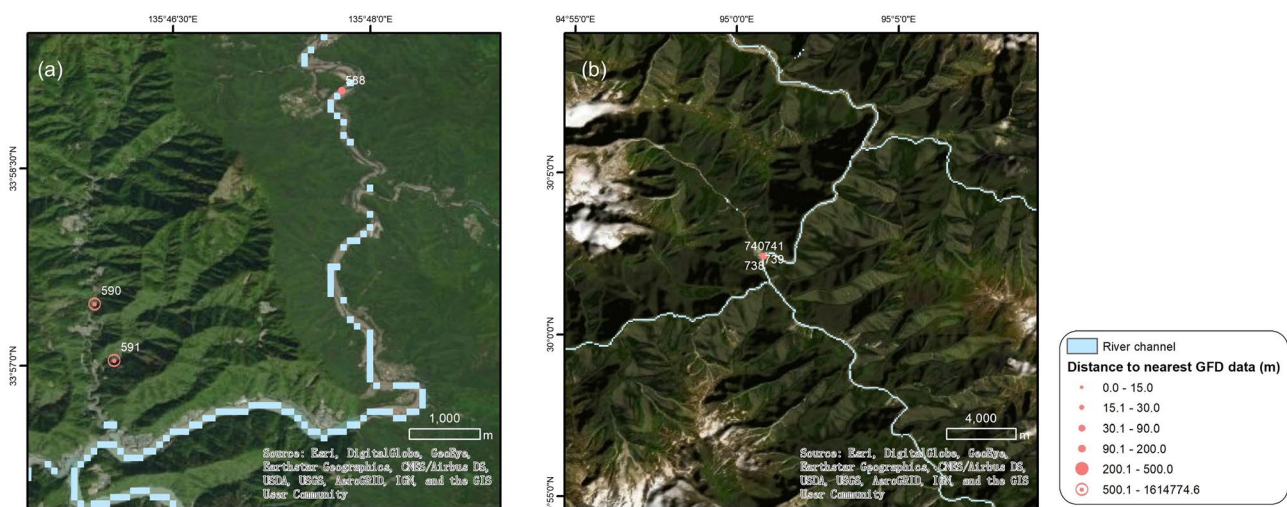
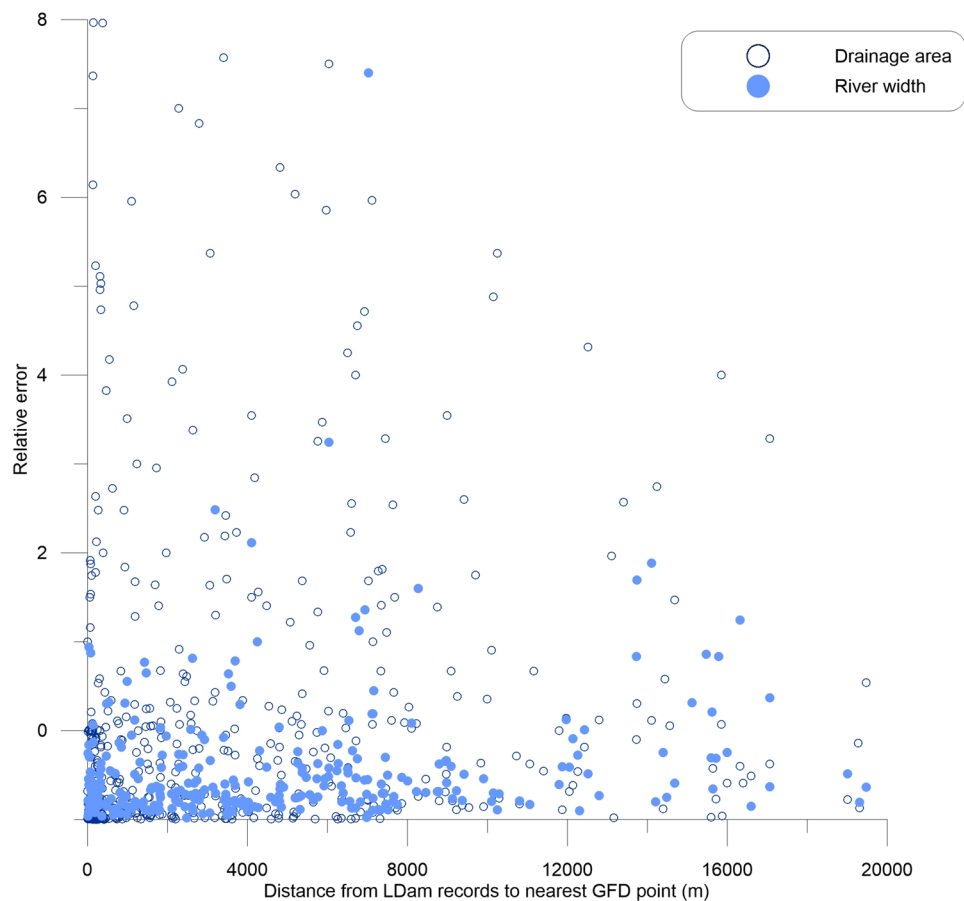


Fig. 11 Examples of uncertainty due to the limitations of GFDs: missing representation of features and inaccurate assembling result due to imprecise location: (a) missing fluvial channel representation in

small catchments; (b) inaccurate data assembling result at the channel junctions due to the imprecision of spatial information

Fig. 12 Correlation between the relative errors of drainage area and river width, and the distance from LDam records to the nearest GFD point



of fluvial related parameters could be inaccurately linked to the main-stream instead of the tributary, if using automated geolocation methods.

In summary, the uncertainty of data from LDam records assembling with GFDs can be summarized into two aspects: (1) the limitations of GFDs; (2) uncertainty caused by geolocated error in the records. To further address which aspect accounts more for the data assembling uncertainties, we apply a measurement called relative error for measuring the data difference between these two datasets. The relative error (δx) is defined as Eq. 3:

$$\delta x = \frac{x - x_0}{x} \quad (3)$$

where x is the data value from original LDam records, x_0 is the estimated value (data from GFDs). The distance from the LDam record to the nearest data point does not proportionally increase with the relative error of drainage area and river width (Fig. 12). The noise observed on the plot suggests that the spatial precision of records may not be the major cause of the data difference.

Conclusions

Linking other additional supplemental data to geolocated LDam datasets was highly recommended in previous LDam research (e.g., Tacconi Stefanelli et al. 2016, 2018; Fan et al. 2020). We have successfully created a geolocated landslide dam inventory and linking the records with other available fluvial data sources to supplement the parameters in the data. Our new global LDam dataset

is called RAGLAD and contains 779 records. The records contain spatial coordinates, time information, dam materials, geomorphological characteristics of catchments, landslides and impounded lakes dimensions, and hydrographic characteristics of subsequent flood events and their consequent damage. The data were compiled from literature in mainly 3 languages. The geospatial accuracy of the records in RAGLAD was enhanced to reduce the uncertainty when linking with global fluvial datasets. RAGLAD can be useful for researchers and global communities to further explore and discuss the LDam formation and risks, and the data are openly available through the authors.

For the first time, we supplement LDam records with auxiliary data from GFDs. The result shows that GFDs can be applied as an acceptable supplement data source for presenting a more comprehensive data distribution of geomorphological parameters. By exploring the limitations, we found that the data difference between actual data and combined data is caused by the poor fluvial channel presentation in small catchments of the GFDs and the uncertainties caused by original records in the data combination. The data combination results can be expected to improve when global datasets improve in the future.

Analysis of the resulting database reveals that LDam records are clustered in the mountainous areas, which is similar to those of general landslides (Nadim et al. 2006; Petley 2012; Froude and Petley 2018). The geomorphological parameter relationships show that the scale exponent difference based on landslide volume and landslide area compared well with those identified in the

previous landslide research. We have also discovered a potential threshold based on the relationship of landslide volume and river width, which could be useful for exploratory LDam formation risk estimation.

This study is the first attempt to publish a global geolocated LDam dataset and link it with global fluvial datasets as a supplement for data gaps in fluvial parameters. Our research also recommends considering the LDam as an independent hazard type, as the landslides that formed LDam have different geomorphological characteristic, such as H/L ratio and landslide volume, compared with general landslides. More efforts are required to study the specific LDam formation triggers and the geomorphological background that shows susceptibility to LDam formation. Additionally, further analysis such as the evaluation of landslide dam formation susceptibility can be carried out based on this dataset.

Acknowledgements

Special thanks go to Stephanie Trigg for providing some cases of landslide dams, Mark Bernhofen for providing the suggestions of global fluvial datasets, and Yanyi Liu for providing some literature of landslide dams in China. We would like to thank Dr Anja Dufresne and another anonymous reviewer who provided constructive reviews for improving this paper.

Author contribution

HW design the study, perform the major jobs of data collection and analysis, and draft of the manuscript; MT contribute to the majority of editing the text; MT, WM, and RF contribute in forming the research objectives, supporting the data analyses and interpretations, manuscript revision.

Funding

Hang Wu received the University of Leeds Scholarship In Associate with the China Scholarship Council (No. 201906400001).

Availability of data and material

All the relevant data are within the manuscript and its supplementary material files. The location of all the landslide dam records and the data gathered from global fluvial datasets are open access for all the academic usage as presented in the supplementary data in shapefile format (RAGLAD_LDam_record_GFD.shp). For more detail information for each landslide dam record, please contact the authors with the landslide dam record index in RAGLAD (RAGLAD basic).

Declarations

Ethics approval Not applicable for this research.

Consent to participate Not applicable for this research.

Consent for publication Not applicable for this research.

Conflict of interest The authors declare no competing interests.

Open Access This article is licensed under a Creative Commons Attribution 4.0 International License, which permits use, sharing, adaptation, distribution and reproduction in any medium or format, as long as you give appropriate credit to the original author(s) and the source, provide a link to the Creative Commons licence, and indicate if changes were made. The images or other third party material in this article are included in the article's Creative Commons licence, unless indicated otherwise in a credit line to the material. If material is not included in the article's Creative Commons licence and your intended use is not permitted by statutory regulation or exceeds the permitted use, you will need to obtain permission directly from the copyright holder. To view a copy of this licence, visit <http://creativecommons.org/licenses/by/4.0/>.

References

- Allen GH, Pavelsky TM (2018) Global extent of rivers and streams. *Science* 361(6402):585–588
- Barla G, Paronuzzi P (2013) The 1963 Vajont Landslide: 50th Anniversary. *Rock Mech Rock Eng* 46(6):1267–1270
- Chunyu D, Selviyan S, Selviyan A (2020) Possible methods analysis and optimization of the landslide slope stabilization in the reconstruction area of the escalator gallery on the Moscow River shore. *IOP Conference Series: Mater Sci Eng* 883
- Costa JE, Schuster RL (1988) The formation and failure of natural dams. *Geol Soc Am Bull* 100(7):1054–1068
- Costa JE, Schuster RL (1991) Documented historical landslide dams from around the world (No. 91–239). <https://pubs.usgs.gov/of/1991/0239/report.pdf>. Accessed 10th Jan 2021
- Clague JJ, Evans SG (1994) Formation and failure of natural dams in the Canadian Cordillera. *Geol Surv Canada Bull* 404
- Dai FC, Lee CF, Deng JH, Tham LG (2005) The 1786 earthquake-triggered landslide dam and subsequent dam-break flood on the Dadu River, southwestern China. *Geomorphology* 65(3–4):205–221
- Davies TR (1982) Spreading of rock avalanche debris by mechanical fluidization. *Rock Mech* 15:9–24
- Davies TR, McSaveney MJ (2012) Mobility of long-runout rock avalanches. *Landslides—types, mechanisms and modeling*. Clague JJ and Stead D (Eds). Cambridge University Press 50–58
- Dufresne A, Geertsema M (2020) Rock slide–debris avalanches: flow transformation and hummock formation, examples from British Columbia. *Landslides*, 17(1):15–32. <https://doi.org/10.1007/s10346-019-01280-x>
- Dunning S. A., Rosser N. J., Petley D. N., Massey C. R. (2006) Formation and failure of the Tsatichhu landslide dam, Bhutan. *Landslides* 3(2):107–113. <https://doi.org/10.1007/s10346-005-0032-x>
- Ermioni L, Casagli N (2003) Prediction of the behaviour of landslide dams using a geomorphological dimensionless index. *Earth Surf Proc Land* 28(1):31–47
- Evans SG, Delaney KB, Hermanns RL, Strom A, Scarascia-Mugnozza G (2011) The formation and behaviour of natural and artificial rockslide dams; implications for engineering performance and hazard management. *Natural and artificial rockslide dams*. Springer, Berlin, Heidelberg, pp 1–75
- Fan X, Dufresne A, Siva Subramanian S, Strom A, Hermanns R, Tacconi Stefanelli C, Hewitt K, Yunus AP, Dunning S, Capra L, Geertsema M, Miller B, Casagli N, Jansen JD, Xu Q (2020). The formation and impact of landslide dams – State of the art. *Earth-Sci Rev* 203
- Fan X, Xu Q, Scaringi G, Dai L, Li W, Dong X, Zhu X, Pei X, Dai K, Havenith H-B (2017) Failure mechanism and kinematics of the deadly June 24th 2017 Xinmo landslide, Maoxian, Sichuan. *China Landslides* 14(6):2129–2146

- Fan XM, Rossiter DG, Van Westen CJ, Xu Q, Gorum T (2014) Empirical prediction of coseismic landslide dam formation. *Earth Surf Proc Land* 39(14):1913–1926
- Fan XM, Van Westen CJ, Xu Q, Gorum T, Dai FC (2012) Analysis of landslide dams induced by the 2008 Wenchuan earthquake. *J Asian Earth Sci* 57:25–37
- Froude MJ, Petley DN (2018) Global fatal landslide occurrence from 2004 to 2016. *Nat Hazards Earth Syst Sci* 18(8):2161–2181
- Frasson RPD, Pavelsky TM, Fonstad MA, Durand MT, Allen GH, Schumann G, Lion C, Beighley RE, Yang X (2019) Global relationships between river width, slope, catchment area, meander wavelength, sinuosity, and discharge. *Geophys Res Lett* 46(6):3252–3262
- Geertsema M (2008) Natural dams, temporary lakes, and outburst floods in Western Canada, The first World Landslide Forum UN/ISDR Tokyo, Japan 211–214
- Geertsema M, Schwab JW, Blais-Stevens A, Sakals ME (2009) Landslides impacting linear infrastructure in west central British Columbia. *Nat Hazard* 48(1):59–72
- Geological Survey (1965) Geological Survey Research 1965. U.S. Government Printing Office, Washington, D.C.
- George DL, Iverson RM, Cannon CM (2019) Seamless numerical simulation of a hazard cascade in which a landslide triggers a dam-breach flood and consequent debris flow, in *Debris-Flow Hazards Mitigation: Mechanics, Monitoring, Modeling, and Assessment*, Proceedings of the Seventh International Conference on Debris-flow Hazards Mitigation, Association of Engineering and Environmental Geologists Special Publication 28, In: Kean J W, Coe JA, Santi PM, Guillen B. K(ed):287–293
- Glastonbury J, Fell R (2008) Geotechnical characteristics of large slow, very slow, and extremely slow landslides. *Can Geotech J* 45(7):984–1005
- Golly A, Turowski JM, Badoux A, Hovius N (2017) Controls and feedbacks in the coupling of mountain channels and hillslopes. *Geology* 45(4):307–310
- Guzzetti F, Ardizzone F, Cardinali M, Rossi M, Valigi D (2009) Landslide volumes and landslide mobilization rates in Umbria, central Italy. *Earth Planet Sci Lett* 279(3–4):222–229
- Hermanns RL, Folguera A, Penna I, Fauqué L, Niedermann S (2011) Landslide dams in the Central Andes of Argentina (Northern Patagonia and the Argentine Northwest), natural and artificial rockslide dams. *Lect Notes Earth Sci* 147–176
- Hirpa FA, Gebremichael M, Over TM (2010) River flow fluctuation analysis: effect of watershed area. *Water Resour Res* 46(12)
- Hsü KJ (1975) Catastrophic debris streams (Sturzstroms) generated by rockfalls. *Geol Soc Am Bull* 86:129–140
- Hungr O, Leroueil S, Picarelli L (2014) The Varnes classification of landslide types, an update. *Landslides* 11(2):167–194
- Iverson RM (1997) The physics of debris flows. *Rev Geophys* 35(3):245–296
- Iverson RM, George DL, Allstadt K, Reid ME, Collins BD, Vallance JW, Schilling SP, Godt JW, Cannon CM, Magirl CS, Baum RL, Coe JA, Schulz WH, Bower JB (2015) Landslide mobility and hazards: implications of the 2014 Oso disaster. *Earth and Planetary Science Letters*, 412: 197–208
- Komac M, Hribernik K (2015) Slovenian national landslide database as a basis for statistical assessment of landslide phenomena in Slovenia. *Geomorphology* 249:94–102
- Korup O (2002) Recent research on landslide dams - a literature review with special attention to New Zealand. *Prog Phys Geog* 26(2):206–235
- Korup O (2004) Geomorphometric characteristics of New Zealand landslide dams. *Eng Geol* 73(1):13–35
- Larsen IJ, Montgomery DR, Korup O (2010) Landslide erosion controlled by hillslope material. *Nat Geosci* 3(4):247–251
- Legros F (2002) The mobility of long-runout landslides. *Eng Geol* 63(3–4):301–331
- Lehner B, Verdin K, Jarvis A (2006) HydroSHEDS technical documentation. World Wildlife Fund US, Washington, DC, pp 1–27
- Li Z, Tang T, Yuan X, Yu G (2020) Impacts of barrier dams blocking the river on morphological processes of upper alluvial channel in Yarlung Tsangpo Grand Canyon Zone. *J Yangtze River Sci Res Inst* 37(8):16–21 (In Chinese, with English title and abstract)
- Linke S, Lehner B, Ouellet Dallaire C, Ariwi J, Grill G, Anand M, Beames P, Burchard-Levine V, Maxwell S, Moidu H, Tan F, Thieme M (2019) Global hydro-environmental sub-basin and river reach characteristics at high spatial resolution. *Sci Data* 6(1):1–15
- Macias JL, Capra L, Scott KM, Espindola JM, Garcia-Palomo A, Costa JE (2004) The 26 May 1982 breakout flows derived from failure of a volcanic dam at El Chichon, Chiapas. *Mexico Geol Soc Am Bull* 116(1–2):233–246
- Miller B, Dufresne A, Geertsema M, Atkinson N, Evensen H, Cruden D (2018) Longevity of dams from landslides with sub-channel rupture surfaces, Peace River region, Canada. *Geoenviro Disasters* 5(1)
- Nadim F, Kjekstad O, Peduzzi P, Herold C, Jaedicke C (2006) Global landslide and avalanche hotspots. *Landslides* 3(2):159–173
- Nash T, Bell D, Davies T, Nathan S (2008) Analysis of the formation and failure of Ram Creek landslide dam, South Island, New Zealand. *N Z J Geol Geophys* 51(3):187–193
- Okura Y, Kitahara H, Kawanami A, Kurokawa U (2003) Topography and volume effects on travel distance of surface failure. *Eng Geol* 67(3–4):243–254
- Perucca LP, Angillieri MYE (2009) Evolution of a debris-rock slide causing a natural dam: the flash flood of Rio Santa Cruz, Province of San Juan-November 12. *Nat Hazards* 50(2):305–320
- Petley D (2012) Global patterns of loss of life from landslides. *Geology* 40(10):927–930
- Roback K, Clark MK, West AJ, Zekkos D, Li G, Gallen SF, Chamlagain D, Godt JW (2018) The size, distribution, and mobility of landslides caused by the 2015 Mw7.8 Gorkha earthquake. *Nepal Geomorphology* 301:121–138
- Robinson TR, Davies TRH, Wilson TM, Orchiston C, Barth N (2015) Evaluation of coseismic landslide hazard on the proposed Haast-Hollyford Highway, South Island, New Zealand. *Georisk: Assessment and Management of Risk for Engineered Systems and Geohazards* 10(2):146–163
- Scheidegger AE (1973) On the prediction of the reach and velocity of catastrophic landslides. *Rock Mech* 5:231–236
- Schuster RL, Costa JE (1986) Perspective on landslide dams. In *Landslide Dams: Processes, Risk, and Mitigation*. Proceedings of a Session in Conjunction with the ASCE Convention, pp 1–20
- Seibert J, McGlynn BL (2007) A new triangular multiple flow direction algorithm for computing upslope areas from gridded digital elevation models. *Water Resour Res* 43(4)
- Shanmugam G, Wang Y (2015) The Landslide Problem *J Palaeogeogr* 4(2):109–166
- Strom A (2010) Landslide dams in Central Asia region. *Journal of the Japan Landslide Society*, 47(6): 309–324
- Tacconi Stefanelli C, Segoni S, Casagli N, Catani F (2016) Geomorphic indexing of landslide dams evolution. *Eng Geol* 208:1–10
- Tacconi Stefanelli C, Vilímek V, Emmer A, Catani F (2018) Morphological analysis and features of the landslide dams in the Cordillera Blanca. *Peru Landslides* 15(3):507–521
- Tarboton DG (1997) A new method for the determination of flow directions and upslope areas in grid digital elevation models. *Water Resour Res* 33(2):309–319
- Wang FW, Zhang YM, Huo ZT, Matsumoto T, Huang BL (2004) The July 14, 2003 Qianjiangping landslide, Three Gorges Reservoir. *China Landslides* 1(2):157–162
- Yamazaki D, Ikeshima D, Sosa J, Bates PD, Allen GH, Pavelsky TM (2019) MERIT hydro: a high-resolution global hydrography map based on latest topography dataset. *Water Resour Res* 55(6):5053–5073
- Yamazaki D, O’Loughlin F, Trigg MA, Miller ZF, Pavelsky TM, Bates PD (2014) Development of the global width database for large rivers. *Water Resour Res* 50(4):3467–3480
- Yin Y, Wang F, Sun P (2009) Landslide hazards triggered by the 2008 Wenchuan earthquake, Sichuan. *China Landslides* 6(2):139–152
- Xu Q, Fan XM, Huang RQ, Westen CV (2009) Landslide dams triggered by the Wenchuan Earthquake, Sichuan Province, south west China. *Bull Eng Geol Environ* 68(3):373–386
- Zhang L, Peng M, Chang D, Xu Y (2016) Dam failure mechanisms and risk assessment. John Wiley & Sons, Singapore
- Zheng H, Shi Z, Shen D, Peng M, Hanley KJ, Ma C, Zhang L (2021) Recent advances in stability and failure mechanisms of landslide dams. *Front Earth Sci* 9

Supplementary Information The online version contains supplementary material available at <https://doi.org/10.1007/s10346-021-01817-z>.

Hang Wu (✉) · **Mark A. Trigg**

School of Civil Engineering, University of Leeds, Leeds, UK
Email: cnhwu@leeds.ac.uk

William Murphy

School of Earth and Environment, University of Leeds, Leeds, UK

Raul Fuentes

Institute of Geomechanics & Underground Technology, RWTH Aachen University, Aachen, Germany